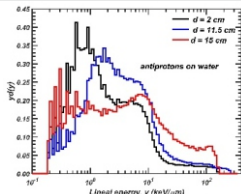# Medical Applications

6

Antiproton Radiotherapy: A Monte Carlo-based Microdosimetric Approach

Arghya Chattaraj and T. Palani Selvam*

Radiological Physics and Advisory Division; Health, Safety & Environment Group, Bhabha Atomic Research Centre, Trombay – 400085, INDIA

Microdosimetric distributions of 126 MeV antiproton at different depths in water

ABSTRACT

Antiprotons are advantageous in radiotherapy as their annihilation physics results in an enhanced energy deposition at tumor location. Further, knowledge on Relative Biological Effectiveness (RBE) and Quality Factor (Q) is important to make a complete assessment on their usefulness in radiotherapy. Microdosiemtric techniques serve as a powerful tool to calculate RBE and Q. These parameters are calculated for 126 MeV antiprotons at 1 μm site size in water using the FLUKA-based Monte Carlo code.

KEYWORDS: *Microdosimetry, Monte Carlo, Antiproton*

Introduction

The goal of the radiotherapy is to deliver high dose to the tumour and spare the surrounding normal tissues. Radiotherapy uses low LET (Linear Energy Transfer) radiations such as ^{60}Co, Mega-voltage X-rays (4–15 MV), Electrons (4–18 MeV) and high LET radiations such as protons and carbon ions. Note that high LET particles have enhanced Relative Biological Effectiveness (RBE) as compared to low LET radiation. The possibility of using antiprotons in radiotherapy is reported in the literature [1-5]. This study focuses on microdosimetry-based investigation of 126 MeV antiprotons for radiotherapy using the Monte Carlo techniques.

What is Antiproton?

Antiproton ($\bar{p}$) is the antiparticle of proton (p). It is a negative heavy ion without any electronic structure. It is discovered by Emilio Segre and Owen Chamberlain in 1955. Antiproton is a spin ½ particle having mass of 938.3 MeV/c^2. The antiprotons are stable, but they are typically short-lived as any collision with proton or neutron will cause annihilation. Antiproton consists of two up antiquarks and one down antiquark ($\bar{p} \equiv uud$). Proton is made of two up quarks and one down quark ($p \equiv uud$). Charge of each quark is 1/3 whereas each antiquark has -1/3. Hence, the electric charge of proton is 1 whereas it is -1 for antiproton. Similarly, magnetic moment of antiproton is negative which is positive for proton.

Production of Antiprotons

Currently few laboratories in the world such as CERN and Fermi National Accelerator Laboratory produce antiprotons [4-7]. CERN produces antiprotons at clinically relevant energies (47 and 126 MeV). The Antiproton Decelerator (AD) at CERN produces low-energy antiprotons for studies of antimatter, and creates antiatoms. The low energy antiproton beam lines at CERN is shown in Fig.1. A 26 GeV/c proton beam from Proton Synchrotron is fired into a block of metal. (typical target is a thin, highly dense rod of iridium metal of 3-mm diameter and 55 cm in length embedded on graphite

enclosed by a sealed water-cooled titanium case). These collisions create a multitude of secondary particles, including antiprotons having different energies. The peak production occurs at antiproton energy of 3.6 GeV. These antiprotons are (a) collected at this production energy in the AD ring, (b) decelerated to lower energies, and (c) cooled using stochastic cooling as well as electron cooling to decrease beam emittance. These antiprotons exit from the accelerator vacuum through a 15 μm titanium window and pass several non-destructive beam monitors before entering the biological target. The total charge extracted from the accelerator can be measured using fast current transformer. Depending on the experimental requirements, the antiproton beam focus can be changed between $r = 4 - 15$ mm.

Interaction of Antiprotons with Matter

At high velocities, antiprotons and protons behave in a similar manner in terms of energy deposition in the medium. However, after slowing down in the medium, antiprotons are captured by a nucleus and annihilate on its surface [2, 8-10]. The basic idea of antiproton radiotherapy is to use the excess

Fig.1: Panoramic view of the low energy antiproton beam lines at CERN (Ref: https://home.cern/news/news/physics/making-antimatter-transportable).

*Author for Correspondence: T. Palani Selvam
E-mail: pselvam@barc.gov.in
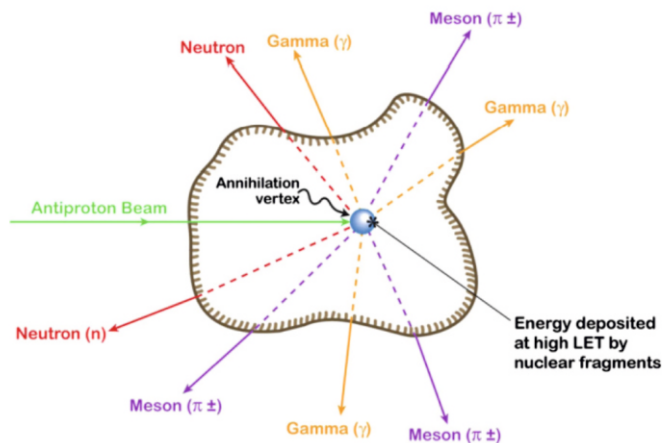
Fig.2: Annihilation event produced by an antiproton stopping in matter [10].

Fig.3: FLUKA-calculated depth–dose profiles in water for 126 MeV antiprotons and protons [6]. The Bragg peak is at 11.5 cm depth.

energy deposited from the antiproton–nucleus annihilation near the Bragg peak. Fig.2 represents annihilation event experienced by an antiproton while stopping in matter. As depicted in Fig.2, during annihilation several secondary particles are produced. In the annihilation process 1.88 GeV (twice proton rest-mass) is released and converted, on average, into 4 - 5 pions (π^+, π^- and π^0).

The average kinetic energy of each Pion is about 300 MeV. The 300 MeV charged Pion has a range of many tens of centimeters in water. π^0 meson is highly unstable and decays instantaneously into high energy gamma-rays with roughly 70–300 MeV. The antiproton can also annihilate by combining with a neutron in nucleus in which the decay products are mostly high energy Pions. Most of the energy produced from the annihilation of antiproton is deposited over a very wide region. Antiproton rarely produces K-meson in antiproton-nucleon annihilation. Mostly 1 or 2 charged Pions penetrate the nucleus and induce an intra-nuclear cascade which results in production of high-LET charged fragments. These fragments have a very short range in the target and will deposit their kinetic energy in the immediate vicinity of the annihilation vertex.

Microdosimetric Quantities

Microdosimetry is evaluation of statistical distribution of energy deposition events at cellular and sub-cellular levels [11]. The microdosimetric quantity, lineal energy, y is defined as $y = \varepsilon / \bar{l}$ where ε is energy imparted to the volume of interest by a single energy deposition event and $\bar{l}$ is the mean chord length [12]. $\bar{l} = 2d/3$, where d is site diameter. $f(y)$ is number of events with event size between y and $y + dy$ and $d(y) = yf(y)/\bar{y}_F$ is dose probability density of y.

Methods and Materials

The present study utilized FLUKA code (version 2011 – 3.0) and considered 126 MeV antiproton beam of 5 x 5 cm^2 field size at the surface of the 20 x 20 x 20 cm^3 water phantom. Absorbed dose in water is scored at various depths along the central axis. Similarly, depth-dose profile of 126 MeV protons is also calculated for a comparison. To calculate on-axis microdosimetric distributions at 1 μm site size, Tissue-Equivalent Proportional Counter (TEPC) is filled with TE-propane gas of density 7.784 x 10^{-5} g/cm^3 and is centered at depths d = 2, 8, 9.5, 11.5 and 15 cm in the water phantom. 10^{10} primary particles are simulated. Using the calculated microdosimetric distributions, *RBE* and *Q* are calculated. The Microdosimetric Kinetic Model (MKM)-based RBE at 10% survival level can be calculated using the equation [12]:
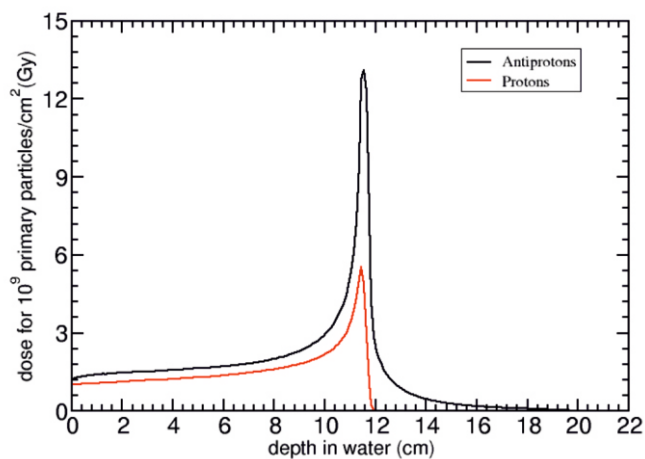
$$RBE = \frac{\sqrt{\alpha_x^2 - 4\beta_x \ln(0.1)} - \alpha_x}{\sqrt{\alpha_t^2 - 4\beta_t \ln(0.1)} - \alpha_t} \times \frac{\beta_t}{\beta_x}$$

Where $\alpha_t = \alpha_0 + \beta_t z^*_{1D}$ and z^*_{1D} is dose-mean specific energy corrected for saturation effect.

The MKM parameters are taken from Kase et al [13] for HSG tumour cell: $\beta_t = \beta_x = 0.05$ Gy^{-2}, α_x(200 kV$_p$ X-rays) = 0.19 Gy^{-1},) r_d = 0.42±0.04 μm, α_0 = 0.13±0.03Gy^{-1}, p = 1 g/cm^3 and y_0 = 150 keV/ μm. Q is calculated using the recommendations of ICRU Report 40 [14].

Depth Dose Profile

Fig.3 presents the on-axis depth-dose profiles of 126 MeV antiprotons and protons in water. The Bragg peak appears at about 11.5 cm for both antiprotons and protons. Note that tumor location coincides with the location of Bragg peak. As compared to protons, dose from antiprotons is higher by a factor of 2.6 and 1.3 at the Bragg peak and in the entrance region, respectively.

Microdosimetric Distribution

The microdosimetric distribution is plot of $yd(y)$ on a linear scale versus y on a log-scale. Fig.4 presents on-axis microdosimetric distributions of 126 MeV antiproton at d = 2, 11.5 and 15 cm in water. As the depth increases from 2 to 11.5 cm, the kinetic energy of antiproton decreases and hence the peak position of the distributions is shifted toward higher
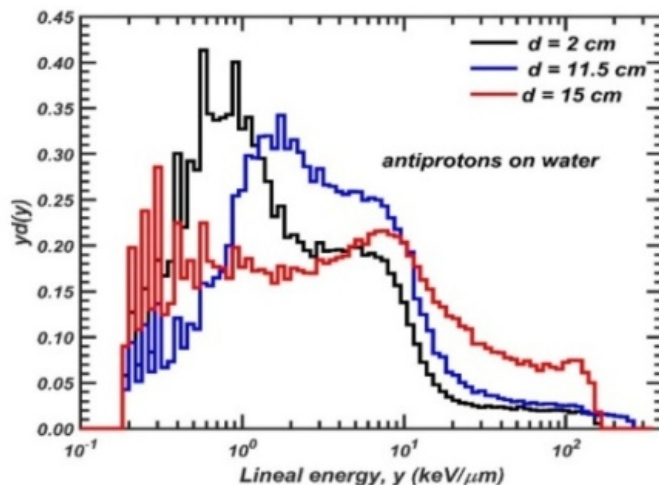

Fig.4: FLUKA-calculated on-axis microdosimetric distributions of 126 MeV antiprotons in water at different depths.

Table 1: Comparison of FLUKA-calculated, values of RBE and $\bar{Q}$ for 126 MeV proton and antiproton.

D	Proton		Antiproton	
(cm)	RBE	$\bar{Q}$	RBE	$\bar{Q}$
2	0.98±0.03	0.95±0.004	1.02±0.03	1.66±0.004
8	0.98±0.03	1.01±0.004	1.02±0.03	1.63±0.004
9.5	0.99±0.03	1.14±0.003	1.07±0.03	2.27±0.003
11.5	1.02±0.03	1.51±0.009	1.27±0.03	5.11±0.009
15	1.40±0.02	6.78±0.007	1.11±0.03	4.09±0.007

y-values. The peak height of the distribution at d = 11.5 cm is smaller than that at d = 2 cm. The long tail part in the distribution at d = 11.5 cm is due to the high-LET radiations generated from the annihilation of antiprotons. The distribution at d = 15 cm is spread over a wide range of y-values and there is no prominent peak.

Table 1 presents the FLUKA-calculated on-axis *RBE* and $\bar{Q}$ values for 126 MeV antiprotons and protons at different depths in water. $\bar{Q}$ and *RBE* of antiprotons and protons are insensitive to depth in the plateau region. At the Bragg peak, values of *RBE* and $\bar{Q}$ of antiprotons are higher by a factor of 1.25 and 3.4, respectively, as compared to protons. The enhancement in RBE and $\bar{Q}$ is significant in terms of radiobiological effects.

Conclusion

The study shows that antiproton radiotherapy is advantageous as compared to protons considering enhancements in the absorbed dose, RBE and $\bar{Q}$ at the Bragg peak. However, the annihilation products of antiprotons such as high energy gamma, pions and neutrons are of great concern in terms of shielding and the associated radiation protection issues. Hence, the technical and economic viability of the application of antiprotons for radiotherapy treatment need to be investigated thoroughly.

References

[1] Gray, L and Kalogeropoulos, T. E. "Possible biomedical applications of antiproton beams: focused radiation transfer" Radiation Research, 1984, 97, 246.

[2] Bassler, N., Holzscheiter, M. H. and Jakel, O. et al. "The antiproton depth-dose curve in water". Physics in Medicine & Biology, 2008, 53, 793–805.

[3] Bassler, N., Hansen, J. W. and Palmans, H. et al. "The antiproton depth–dose curve measured with alanine detectors". Nuclear Instruments and Methods in Physics Research Section B, 2008, 266, 929-36.

[4] Bassler, N., Alsner, J., Beyer, G. et al. "Antiproton radiotherapy". Radiotherapy and Oncology, 2008, 86, 14-9.

[5] Holzscheiter, M. H., Agazaryan, N. and Bassler, N. et al. "Biological effectiveness of antiproton annihilation". Nuclear Instruments and Methods in Physics Research Section B, 2004, 221, 210-4.

[6] Chattaraj, A. and Selvam, T. P. "Comparison of 126 MeV antiproton and proton – a FLUKA-based microdosimetric approach". Physics in Medicine & Biology, 2022, 67, 185014

[7] Jackson, G. P. "Practical Uses of Antiprotons". Hyperfine Interactions, 2003, 146/147, 319-23.

[8] Inokuti, M. "Interactions of antiprotons with atoms and molecules". Nuclear Tracks in Radiation Measurements, 1989, 16, 115-23.

[9] Lewis, R. A., Smith, G. A. and Howe, S. D. "Antiproton portable traps and medical applications". Hyperfine Interactions, 1997, 107, 155-64.

[10] Hall, E. J. "Antiprotons for radiotherapy?". Radiotherapy and Oncology, 2006, 81, 231-2.

[11] ICRU. "Microdosimetry". ICRU report 36 (Bethesda, MD: ICRU), 1983.

[12] Newpower, M., Patel, D. and Bronk. L. et al. "Using the Proton Energy Spectrum and Microdosimetry to Model Proton Relative Biological Effectiveness". International Radiation Oncology Biology Physics, 2019, 104(2), 316-24.

[13] Kase, Y., Kanai, T., Matsumoto, Y. et al. "Microdosimetric Measurements and Estimation of Human Cell Survival for Heavy-Ion Beams". Radiation Research, 2006, 166, 629-38.

[14] ICRU. "The quality factor in radiation protection" ICRU Report 40 (Bethesda, MD: ICRU), 1986.